21.3 A CMOS Multi-Functional Biosensor Array for Rapid Low-Concentration Analyte Detection with On-Chip DEP-Assisted Active Enrichment and Manipulation with No External Electrodes

Dongwon Lee[1], Doohwan Jung[2], Fuze Jiang[1], Gregory Villiam Junek[3], Jongseok Park[4], Hangxing Liu[1], Ying Kong[1], Youngin Kim[1], Jing Wang[1], Hua Wang[1,3]

[1]ETH Zürich, Zurich, Switzerland, [2]Qualcomm, San Jose
[3]Georgia Institute of Technology, Atlanta, GA, [4]Apple, San Diego, CA

Electronic biosensors are transducers that convert biomolecular or cellular information to electronic readouts. Though advances in electronics keep improving biosensors' performance, often their ultimate detection limits and functionalities are constrained at the sensor interfaces. For instance, existing electrochemical or optical bioanalytical platforms commonly face challenges in immobilizing surface bioreceptors and detecting ultra-trace biospecimens due to the slow mass transport limitation from the bulk solution. Additional target amplification or complex signal enhancement are thus needed. Therefore, there is a perennial need to explore biology-electronics co-designs to overcome some of these interface limitations and further advance biosensor detection capabilities.

One attractive molecular/cellular manipulation technique is dielectrophoresis (DEP) that applies active analyte transport to address interface limitations. Some early CMOS sensor platforms explore DEP on-chip [1-3]. However, they often require external electrodes or cover electrodes, such as ITO electrodes to drive DEP, making the chip packaging difficult and unreliable. Moreover, these reported CMOS DEP chips only contain impedance sensing modality, which limits their functionalities. We propose a DEP-assisted CMOS multi-functional molecular sensor platform for enhanced analyte detection without external electrodes or conductive covers. The on-chip DEP performs manipulation and enrichment of analytes, ensuring fast and reliable low-concentration detections, ideal for rapid sample-in-answer-out environmental monitoring and point-of-care (PoC) devices. Each sensing pixel contains independently controllable and functional three photodiodes, and one in-pixel working electrode (WE) shared by DEP, impedance mapping, and electrochemical modalities and DEP actively transport target analytes to the interface for enhanced detections (Fig. 21.3.1). First, the EC sensors and DEP together achieve higher limit-of-detection (LoD). Since on-chip DEP achieves active transport and analyte enrichment, the EC sensors thus can detect the low concentration analyte. Also, thanks to the DEP-based enrichment, the impedance and EC sensors achieve rapid analysis. Lastly, the DEP-based particle manipulations is readily detected by on-chip optical sensor arrays to ultimately achieve close-loop manipulation and sensing, such as droplet microfluidics.

The physical principle of DEP-based active transport is introduced in Fig. 21.3.1 [4]. An external actuation electrical field will polarize the particles/samples. Strong electrical field and particles with high polarizability make the DEP potential energy magnitude higher and facilitate particle trapping and controlling. If DEP potential energy magnitude is higher than its thermal energy, particles can be manipulated by DEP. However, if the thermal energy is higher than the DEP potential energy magnitude, the Brownian motion is dominant, rendering the DEP manipulation less effective. To yield strong polarization electrical field, our proposed CMOS sensor platform applies differential AC actuation voltages across two adjacent working electrodes (WEs), while the spacing of WEs are carefully designed to ensure sufficient DEP polarization. Note the on-chip DEP reuses the same WEs for electrochemical potentiostats and impedance mapping for area saving, and no external electrode is needed.

Our CMOS biosensor platform contains 4096 WEs, each of 28μm × 28μm. The edge-to-edge spacing between WEs is 22μm. The relative permittivity and conductivity of water are used in simulations. Also, the temperature and polarizability of particles are set up as 298K and 50 x 10^{-31}Fm^2. It should be mentioned that media with low-ionic concentrations enhance DEP polarization, while many molecular and bacteria sensing can be performed in such media and oil-droplet based microfluidics [5, 6]. Our platform uses CMOS-compatible $3V_{p\text{-}p}$ swing with opposite phases on each WE for DEP polarization. The simulation result shows that our design is capable of trapping and manipulating analytes for active transport and enrichment up-to 37μm above the WEs.

Our DEP-assisted CMOS sensor array chip is shown in Fig. 21.3.2. The array chip contains four pixel groups. Each pixel group is made of 1024 28μm x 28μm WEs, 320 28μm x 28μm counter electrodes (CE), 64 28μm x 28μm reference electrodes (RE), and 3072 photodiodes (PD). Also, each pixel group has a programmable DEP controller, an impedance sensing block, an EC potentiostat, 4 optical detection blocks, and 4 programmable output stages. The impedance sensing block makes excitation signals in five frequency levels from 15kHz to 500kHz. The internal digital switch logic and PD-reset logic are also integrated.

To demonstrate the DEP-assisted multi-functional analyte sensing of our CMOS biosensor array, we perform the following biosensing experiments.

We first utilize the resazurin (RS) redox process as a biomarker to detect the presence of living *E. coli* bacteria for rapid environment monitoring and food safety screening (Fig. 21.3.3). The reduction of RS is due to the loss of an oxygen atom loosely bound to the nitrogen atom of the phenoxazine nucleus. The reduction process follows two steps that are observed by cyclic voltammetry (CV) using on-chip potentiostat sensing modality. Firstly, the weakly fluorescent RS is irreversibly reduced into resorufin by the presence of the living *E. coli* bacteria. This step generates the main reduction peak current in CV. The resorufin can be further reduced into dihydroresorufin, observable as the second weaker reduction current peak. This second step is also reversible by atmospheric oxygen. Without *E. coli*, the reduction peak current of RS stays constant over time. In comparison, a clear and time-dependent decrease of amperometric peak current indicates the irreversible reduction of RS caused by living *E. coli*. This enables the rapid detection of living *E. coli* bacteria using our on-chip EC sensors. We load 2 x 10^7 copies/ml *E. coli* with 250μM RS onto our CMOS sensor and conduct CV measurement over 40 minutes. The CV readout shows that our platform can clearly detect the reduction current of RS. Also, CA measurements in Fig. 21.3.3 show the reduction peak current continuously decreases over time, demonstrating rapid living *E. coli* detection by the on-chip EC potentiostat in our CMOS sensor array.

Many biosensing applications require detections of low-concentration targets/analytes and high dynamic range. An example is water quality monitoring when *E. coli* bacteria concentration is low in clean drinkable water. In this case, most sensing platforms cannot yield conclusive results without long sensing time, e.g., for the *E. coli* to diffuse to the sensor surface or for *E. coli* proliferation. These LoD sensor issues can be solved by DEP-based analyte enrichment (Fig. 21.3.4). We label *E. coli* with 2μm-diameter anti-*E. coli* antibodies modified microbeads to show the DEP-based enrichment and the rapid detection. The DEP force acts on the microbeads that actively concentrate *E.coli* bacteria onto WEs and enhance the detection signal. In the experiment, 1kHz DEP actuation voltage is applied to the target electrode array. The measured time-lapse image of DEP-based enrichment is shown. The microbeads are rapidly enriched in the DEP-applied region. The CV scanning is conducted using the WEs both inside and outside of the DEP-applied region. The CV readout shows that the reduction peak current of the DEP-applied region decreases faster than that outside of DEP region. This demonstrates that our DEP-assisted biosensor platform can radically improve the detection speed and LoD (also dynamic-range) for low-concentration analytes.

Figure 21.3.5 shows the joint operation of DEP with the PD optical detection and impedance sensor. First, we demonstrate on-chip sample manipulation by reprogrammable DEP that is further monitored by on-chip PD sensor array. 100μm-diameter polystyrene microbeads are moved in X-/Y-directions by reprogrammable on-chip DEP forces. The bead movements are accurately tracked by PD arrays, which well match the reference microscopic images. Also, for the impedance sensing with DEP, DEP enrichment and impedance mapping are performed both at 15kHz. The 2D impedance change and the microscopic images show that enriched *E. coli* and microbeads are accurately detected by the impedance sensing block. These on-chip optical and impedance detections jointly with on-chip programmable DEP manipulation shows the capabilities of self-contained DEP analyte manipulation with multi-functional biosensing, useful for applications like automated large-scale tissue engineering and cell manufacturing.

Figure 21.3.7 shows our DEP-assisted multi-functional CMOS biosensor array chip in a standard 130nm BiCMOS process. The chip area is 7mm × 7mm and the active sensing area is 3.6mm × 4mm. Our in-house post-processing techniques deposit Ti/Ag on REs and Ti/Au on WEs/CEs for full biocompatibility. The state-of-the-art DEP-assisted CMOS biosensors and CMOS EC biosensors are summarized in Fig. 21.3.6 [7, 8]. Our array platform offers in-pixel multi-functional sensing modalities and supports analyte enrichment and manipulation without any external electrodes or conductive covers.

References:

[1] Y. H. Ghallab and Y. Ismail, "CMOS Based Lab-on-a-Chip: Applications, Challenges and Future Trends," *IEEE Circuits and Systems Magazine*, vol. 14, no. 2, pp. 27-47, 2014, doi: 10.1109/MCAS.2014.2314264.

[2] Chung, Jaehoon, Yu Chen, and Seong-Jin Kim. "High-density impedance-sensing array on complementary metal-oxide-semiconductor circuitry assisted by negative dielectrophoresis for single-cell-resolution measurement." *Sensors and Actuators B: Chemical* 266 (2018): 106-114.

[3] A. Romani et al., "Capacitive sensor array for localization of bioparticles in CMOS lab-on-a-chip," *ISSCC*, pp. 224-225, Feb. 2004.

[4] Taher Ghomian et al., "High-Throughput Dielectrophoretic Trapping and Detection of DNA Origami." *Advanced Materials Interfaces* 8.5 (2021): 2001476.

2023 IEEE International Solid-State Circuits Conference (ISSCC) | 978-1-6654-9016-0/23/$31.00 ©2023 IEEE | DOI: 10.1109/ISSCC42615.2023.10067525

Authorized licensed use limited to: Georgia Institute of Technology. Downloaded on August 03,2023 at 23:28:49 UTC from IEEE Xplore. Restrictions apply.

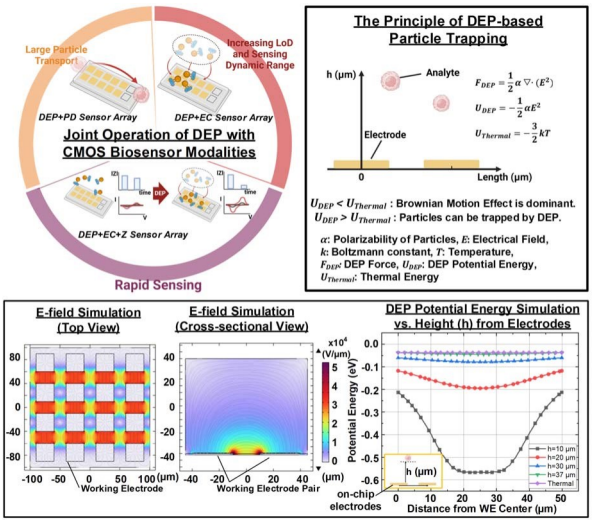

Figure 21.3.1: The joint operation of on-chip electrochemical potentiostat, impedance sensor, and photo diode (PD) array with on-chip DEP as well as the physical principle of DEP-based analyte manipulation, trapping, and enrichment and COMSOL simulations of on-chip DEP functionality.

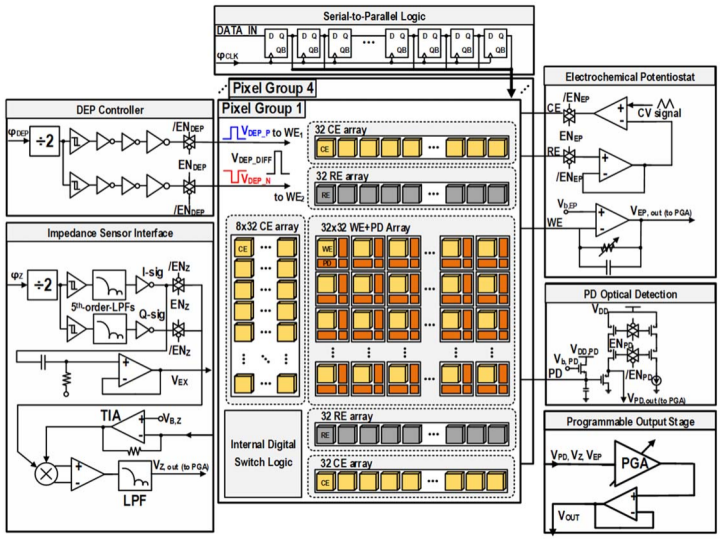

Figure 21.3.2: Circuit schematics and system architecture of DEP-assisted multi-functional CMOS biosensor array platform.

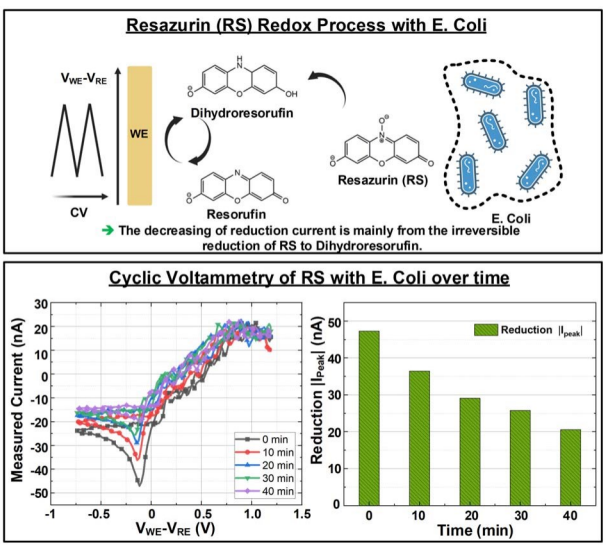

Figure 21.3.3: Detection of live E. coli using Resazurin (RS) redox process and cyclic voltammetry measurement results for live E. coli detection at 2 x 10^7 copies/ml with 250μM RS.

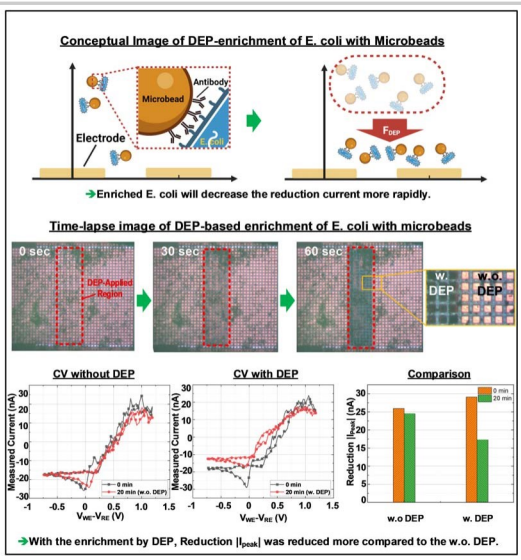

Figure 21.3.4: The DEP-based analyte enrichment and its demonstration to achieve rapid electrochemical detection of low-concentration E. coli, achieving fast, reliable, and high dynamic range biosensors.

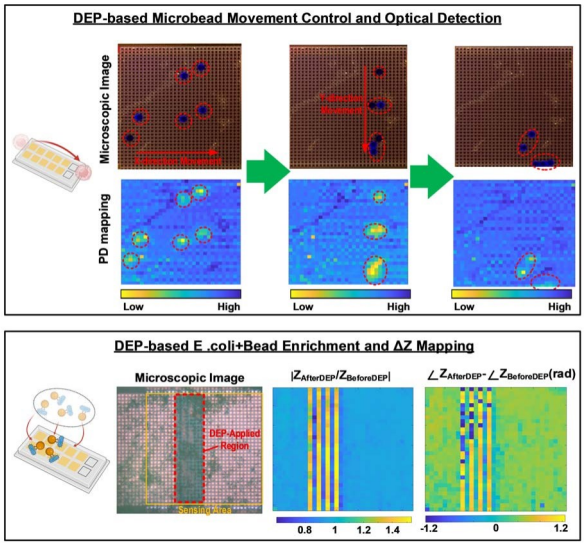

Figure 21.3.5: Joint multi-functional analyte sensing by optical detection with DEP-based analyte manipulation and 2D impedance mapping with DEP-based analyte enrichment.

	This Work	Sen.B 2018 J. Chung [2]	ISSCC 2004 A. Romani [3]	ISSCC 2020 D. Jung [7]	ISSCC 2019 A. Manickam [8]
Modality	Electrochemical + Impedance +PD+ DEP	Impedance + DEP	Capacitive Sensor + DEP	Electrochemical + Impedance Sensing	Electrochemical
DEP actuation	on-chip Electrode (No external cover)	Double Layer with external ITO cover	Double Layer with external ITO cover	No	No
DEP demonstration	1. Bacteria Enrichment 2. Particle Movment Control (X and Y-direction)	Cell Localization	Microbead Localization	-	-
DEP joint function	1. Boost LoD and detection speed of EC/Z sensor 2. Particle Movement control and detection	Boost LoD of Z sensor	Boost LoD of capacitive sensor	-	-
Bio-measurement	Bacteria Detection	MCF Cell impedance Measurement	-	Bacteria Detection	-
Pixel area ($μm^2$)	28 x 28	14 x 14	20 x 20	44 x 52	100 x 100
Electrode material	WE, CE: Ti/Au RE: Ti/Ag	Ti/Au	N/A	WE, RE, CE: Ti/Au	Al/Ti/a-C
Field of View (mm^2)	3.6 x 4.0	3.12 x 3.12	6.4 x 6.4	3.2 x 3.72	3.2 x 3.2
Number of pixels	WE: 4096 RE: 256 CE: 1280	104 x 104	320 x 320	WE: 512 RE: 16 CE: 32	WE: 1024 RE: 1 CE: 1
Imax (nA)	60	N/A	N/A	59.9	12.5
Sensitivity (pA)	2	N/A	N/A	2	0.28
Readout Speed (Hz)	1000k	-	-	1000k	50
Z spectroscopy range (Hz)	15k-500k	100k-1M	N/A	15k-500k	-
Power (mW)	3/pixel group	N/A	N/A	2.25/pixel group	0.25/pixel
CMOS process (nm)	130	180	350	130	250

Figure 21.3.6: Comparison table with the state-of-the-art DEP-integrated CMOS sensors and CMOS electrochemical sensors.

Authorized licensed use limited to: Georgia Institute of Technology. Downloaded on August 03,2023 at 23:28:49 UTC from IEEE Xplore. Restrictions apply.

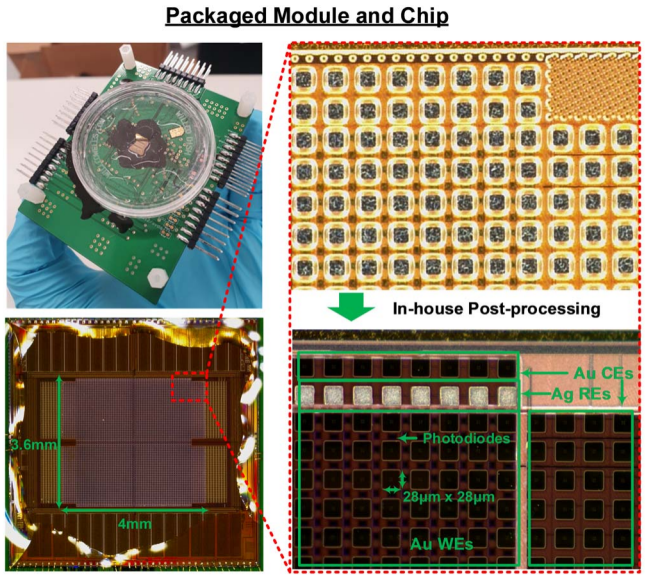

Figure 21.3.7: Packaged module and chip micrographs before and after in-house post-processing.

Additional References:

[5] J.D. Besant et al., "Rapid electrochemical phenotypic profiling of antibiotic-resistant bacteria." *Lab on a Chip* 15.13 (2015): 2799-2807.

[6] S. Kuss et al., "Versatile electrochemical sensing platform for bacteria." *Analytical chemistry* 91.7 (2019): 4317-4322.

[7] D. Jung et al., "28.4 A CMOS Multimodality In-Pixel Electrochemical and Impedance Cellular Sensing Array for Massively Paralleled Synthetic Exoelectrogen Characterization," *ISSCC*, pp. 436-437, Feb. 2020.

[8] A. Manickam et al., "11.2 A CMOS Biosensor Array with 1024 3-Electrode Voltammetry Pixels and 93dB Dynamic Range," *ISSCC*, pp. 192-193, Feb. 2019.

Authorized licensed use limited to: Georgia Institute of Technology. Downloaded on August 03,2023 at 23:28:49 UTC from IEEE Xplore. Restrictions apply.

978-1-6654-9016-0/23/$31.00 ©2023 IEEE